

THEORETICAL PREDICTION OF VOLUMETRIC MASS TRANSFER COEFFICIENT ($k_L a$) FOR DESIGNING AN AERATION TANK

Pisut Painmanakul^{1*}, Jidapa Wachirasak¹,
Marupatch Jamnongwong² and Gilles Hébrard²

¹ Department of Environmental Engineering, Faculty of Engineering
Chulalongkorn University, Bangkok, Thailand 10330

² Laboratoire d'Ingénierie des Systèmes Biologiques et des Procédés,
UMR INSA-INRA 792, Institut National des Sciences
Appliquées de Toulouse, Toulouse, France 31077

Email: pisut.p@chula.ac.th^{1*}, jida.w@hotmail.com¹, marupatch@hotmail.com²
and gilles.hebrard@insa_toulouse.fr²

ABSTRACT

The objective of this present paper is to propose a new theoretical prediction method of the volumetric mass transfer coefficient ($k_L a$) occurring in a gas-liquid contactor based on the dissociation of the liquid-side mass transfer coefficient (k_L) and the interfacial area (a). The calculated results have been compared with those obtained with the experimental process in a small-scale bubble column. Tap water was used as liquid phase and an elastic membrane with a single orifice as gas sparger. Only the dynamic bubble regime was considered in this work ($Re_{OR} = 150-1000$ and $We = 0.002-4$).

This study has clearly shown that, whatever the operating conditions under test, the generated bubble diameters (d_B), bubble frequency (f_B) and their associated rising velocities (U_B) were the important parameters in order to predict, not only the values of $k_L a$, but also the values of a and of k_L . Moreover, these obtained results could provide a better understanding of the parameters which influence the oxygen transfer mechanism in the aeration process. By using the correlations to estimate these bubble hydrodynamics (d_B and U_B), it diminishes times for measuring the associated mass transfer parameters and also their experimental complexities and errors.

KEYWORDS

prediction method, volumetric mass transfer coefficient, interfacial area, liquid-side mass transfer coefficient, bubble diameter, bubble rising velocity

I . Introduction

For the different biological processes (wastewater treatment or fermentation) and chemical oxidation processes, the aeration systems can transfer oxygen into a liquid phase by either diffusing gas through a gas-liquid interface or dissolving gas into the liquid solution by using a semi-permeable membrane [1]. Normally, the gas-liquid interfacial area; which is created by either shearing the liquid surface with a mechanical aerator (mixer or turbine) or releasing air through spargers or porous materials, is applied as the reliable environmental technologies. With the punctured flexible rubber membranes sparger used in wastewater aeration tank, a uniform size distribution of small bubbles is produced and leads to a large mass transfer area [2], without the clogging problems which are normally found with another type of diffusers. Several works have been carried out on the membrane characterization (physical properties) and the bubbles generation phenomena [3] - [8]. In particular, it is interesting to note that the interfacial area (a) can be experimentally determined by using the bubble size (d_B), bubble formation frequency (f_B), bubble rising velocity (U_B) and also the bubble eccentricity (E) [9], [10].

When designing and applying the aeration systems, it is frequently necessary to be able to calculate the volumetric mass transfer coefficient ($k_L a$). A better forecast of the $k_L a$ value would help the optimization of the installations in term of both cost and effectiveness. The $k_L a$ value in gas-liquid contacting equipment has mostly been determined by the oxygen physical absorption or desorption technique (classical method) [11] leading to empiric correlations where $k_L a$ is predicted versus operating parameters without take into account physical phenomenon; in that case the scale up is failing. However, in the actual large-scale aeration system, the application of the existing method for $k_L a$ determination can be limited by various factors such as absorption rate of oxygen from air, complicated operating conditions, measuring equipment quality and cost, and also operator skills. It also fails to take into account all the parameters affecting mass transfer, like tank geometry and layout of the aeration system [12]. In addition, the obtained $k_L a$ values are often global (25% errors values) and insufficient to understand the oxygen mass transfer mechanisms that directly affect the oxygen transfer performance [13], [14]. Therefore, a theoretical way to predict the quick and accurate value of the $k_L a$ coefficient could be interesting for wastewater companies. Moreover, their work underline that it is essential to separate the parameters, especially the liquid-side mass transfer coefficient (k_L) and the interfacial area (a) [15] - [20]. to well predict and be able to scale up the $k_L a$ values obtained. So their data and their conclusions will be reused in this publication to build a new theoretical prediction of $k_L a$ from bubble hydrodynamics (d_B , U_B and f_B) and liquid side mass transfer coefficient k_L .

Concerning to the prediction of the value of $k_L a$ in the aeration system, many correlations and calculating model are available in litterature [11], [21]. However few of them proposed a physical prediction based on the interfacial area and liquid mass transfer coefficient. The original idea of this work is to suppose that value of $k_L a$ can be determined if one knows how to estimate the k_L coefficient and the value of a , individually.

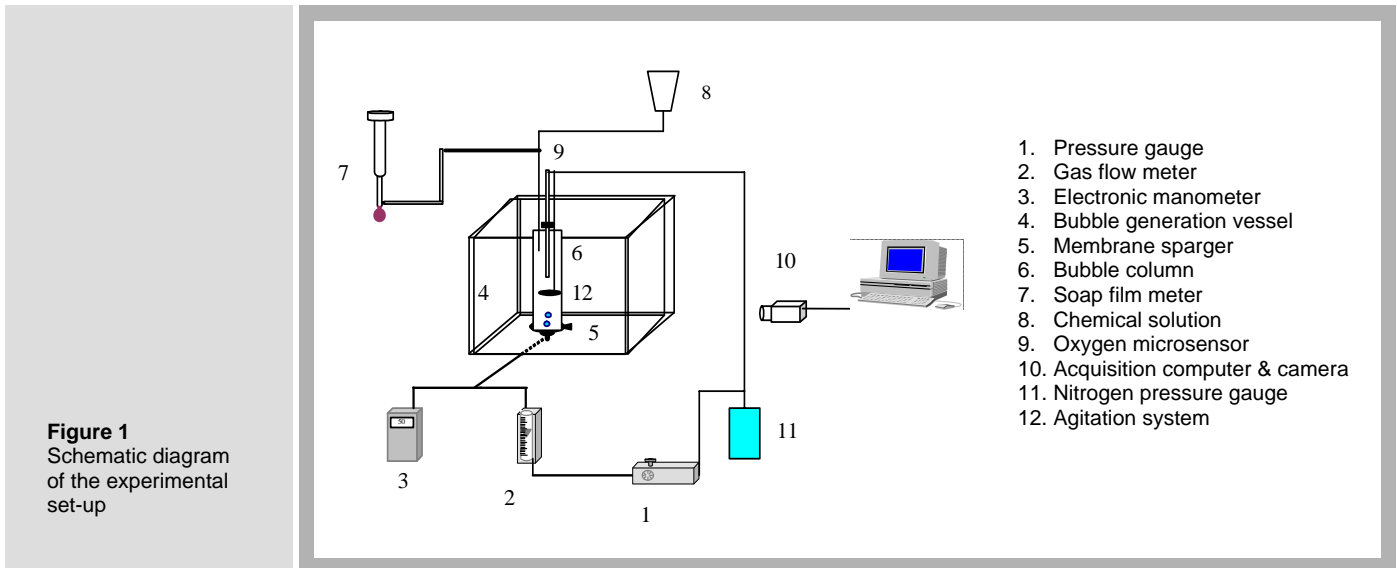
Therefore, the general aim of this paper is to propose a simple theoretical $k_L a$ prediction method based on the determination of k_L and a : the generated bubble sizes will be used as the key factor. The scope of this work is as follows:

- Application of the local experimental method to determine the bubble hydrodynamic (d_B , f_B and U_B) and the mass transfer parameters (a , $k_L a$ and k_L). Note that this applied method enables the mass transfer efficiency to be effectively controlled whatever the operating conditions;
- Proposition of the developed $k_L a$ prediction method that take into account both interfacial area and liquid-side mass transfer coefficient, along with the existing correlation used in the literature;
- Validation of the proposed method by comparing the results obtained with the existing correlation and the local experimental approaches.

According to the outline of this paper, it will firstly present the material and the experimental methods for determining the bubble hydrodynamic and the local mass transfer parameter used in this study. Then, the developed $k_L a$ prediction technique will be described along with the existing correlations used in the calculation of bubble diameters, bubble rising velocity and the k_L coefficient. For the last section, the results obtained with the proposed theoretical method will be compared with those obtained with the existing correlations in terms of the bubble hydrodynamic (d_B and U_B) and the mass transfer parameters (a , $k_L a$ and k_L), and then will also be validated with those obtained experimentally in this study.

II. Material and Experimental Methods

2.1 Experimental set-up



According to [9], [10], the experimental set-up used in this study was applied as in Figure 1. These experiments were carried out in a glass bubble column (6), 0.05 m in diameter, 0.40 m in height. This column was fixed into a glass parallelepiped vessel (4) that has the size of 0.40 m width, 0.40 m length and 0.30 m height. The pressure gauge (1) and gas flow meter (2) were applied in order to monitor the flow of air. The electronic manometer called BIOBLOCK 915PM247 (3) and soap film meter (7) were used for determining the pressure drop from membrane sparger with a single orifice (5) and the average gas flow rate, respectively. Nitrogen gas was used for oxygen elimination in the system and was controlled by a pressure gauge (11). The UNISENSE oxygen microsensor with response time as low as 50 ms was used to measure the change in dissolved oxygen concentration (9). All chemical solutions (8) were injected at the top of the column. Tap water was used as liquid phase with the liquid height $H_L = 25$ cm and temperature $T = 20^\circ\text{C}$. Note that the static and the dynamic bubbling regimes can be observed in this study due to the associated hole diameter ($0.13 < d_{OR} < 0.32$ mm) and gas flow rate ($0.3 < Q_G < 3.45$ ml/s.). Complementary information can be found [9], [10], [22].

2.2 Method for determining the hydrodynamic parameter

The bubble diameters (d_B), the bubble formation frequency (f_B) and the terminal rising velocities (U_B) are determined by image analysis. These parameters are measured at 10 cm above the gas hole. Images are taken with a Leutron LV95 camera ($120 \text{ frames}\cdot\text{s}^{-1}$) and visualized on the acquisition computer through the Leutron vision software. The image treatment is performed with the Visilog 5.4 software (more details can be found in [9]). Note that, in order to get statistically significant distribution, the average bubble diameter (d_B) presented in this study is deduced from the measurement of 150–200 bubbles [22].

The bubble formation frequency (i.e. the number of bubbles formed at the membrane orifice per unit time) is determined as [9]. Note that the quasi-constant bubble size generated was required for this equation. So, assuming that a dispersed bubble population is provided supposed to modify the equation (1).

$$\left(f_B = \frac{Q_G}{V_B} = \frac{N_{OR} \times q}{V_B} \right) \quad (1)$$

where V_B is the average detached bubble volume and Q_G is the gas flow rate measured using the soap film meter. N_{OR} is the number of orifices located on the membrane and is equal to 1 in this study. Thus, q is the mean gas flow rate through each orifice, assuming uniform flow distribution and is similar to Q_G .

Thanks to the image treatment system, the terminal rising bubble velocities, U_B , can be estimated as the distance covered by the bubble between two frames.

$$\left(U_B = \frac{\Delta D}{T_{frame}} \right) \quad (2)$$

where ΔD is the bubble spatial displacement between $t = 0$ and $t = T_{frame} = 1/120$ s.

2.3 Mass transfer parameter determination

In this study, the local experimental approach presented in [23] is used to firstly determine the local interfacial area by using the bubble hydrodynamic parameters, and also the corresponding volumetric mass transfer coefficient. Thus, the local liquid-side mass transfer coefficient can be calculated.

Local interfacial area (a)

As in [9], the interfacial area is a function of the bubble formation frequency, the terminal bubble rising velocity and the generated bubble diameter. It can be expressed as:

$$\left(a = f_B \times \frac{H_L}{U_B} \times \frac{S_B}{V_{Total}} = \frac{N_{OR} \times q}{V_B} \times \frac{H_L}{U_B} \times \frac{\pi \cdot d_B^2}{AH_L + N_B V_B} \right) \quad (3)$$

Local volumetric mass transfer coefficient

The $k_L a$ determination method used in this study is the new one proposed by [22]. This method is based on a mass balance on sulfite sodium (Na_2SO_3) concentration during aeration time. It can be noted that no models for the mixing in the liquid or the gas phase are required. For this method, the local volumetric mass transfer coefficient, $k_L a$, is expressed as:

$$\left(k_L a = \frac{\frac{1}{2} \frac{M_{O_2}}{M_{Na_2SO_3}} m_s}{t_{aeration} V_L C_L^*} \right) \quad (4)$$

where M_{O_2} is the molecular mass of oxygen, $M_{Na_2SO_3}$ the molecular mass of sodium sulfite, m_s the mass of Na_2SO_3 reacting with the oxygen dissolved during the steady state regime, $t_{aeration}$ the aeration time, V_L the liquid volume in the bubble column, and C_L^* the saturation oxygen concentration in the liquid.

Liquid-side mass transfer coefficient (k_L)

The volumetric mass transfer coefficient, $k_L a$, is the product of the liquid-side mass transfer coefficient, k_L , and the interfacial area, a . The local liquid-side mass transfer coefficient is simply determined by:

$$\left(k_L = \frac{k_L a}{a} \right) \quad (5)$$

In this work, these two values are experimentally obtained simultaneously in local conditions, giving a good accuracy. The average and the maximum experimental error for determining the k_L value have been estimated at $\pm 15\%$ and $\pm 30\%$, respectively.

III. Method for Predicting Volumetric Mass Transfer Coefficient ($k_L a$)

In this part, the existing correlations and models for determining the bubble hydrodynamic (d_B and U_B) and also the liquid-side mass transfer coefficient (k_L) provided in a bubble

column are firstly presented. Then, the proposed theoretical $k_L a$ prediction method will be described.

Note that many of these existing correlations were taken from secondary sources recommending their general application, principally because of their theoretical support behind the correlations. Moreover, these equations are normally developed from non-dimensional analysis, and fitted parameters to their correlation in the small-scale experiments: small effective limits placed on the resulting application can be assumed.

3.1 Existing correlations for hydrodynamic and mass transfer parameters

Table 1 and 2 present the correlations used in this evaluation for bubble diameter (d_B) and for their associated rising velocity (U_B) respectively.

Eq.	Correlation	Conditions	Reference
d_B-1	$d_B = \left(\frac{6d_{OR}\sigma g_c}{g\Delta\rho} \right)^{1/3}$	$Q_{go} < \left[\frac{20(\sigma d_0 g_c)^5}{(g\Delta\rho)^2 \rho_L^3} \right]^{1/6}$	Van Krevelen [24]
d_B-2	$d_B = 0.0287 d_{OR}^{1/2} Re^{1/3}$	Re < 2100	Leibson [25]
d_B-3	$d_B = \left(\frac{72\rho_L}{\pi^2 g\Delta\rho} \right)^{1/5} Q_{go}^{0.4}$		Van Krevelen [24]
d_B-4	$d_B = 1.7 \times 10^{-4} \Delta P^{0.328}$	ΔP in Pa	Hebrard [26]
d_B-5	$d_B = 15.73 \times 10^{-3} D_c^{0.32} \left(\frac{Q_g}{A_{BC}} \right)^{0.16}$		Hebrard [26]
d_B-6	$d_B = 1.56 Re^{0.058} \left(\frac{d_{OR}^2 \sigma}{\Delta\rho g} \right)^{1/4}$ $d_B = 0.32 Re^{0.425} \left(\frac{d_{OR}^2 \sigma}{\Delta\rho g} \right)^{1/4}$	1 < Re < 10 10 < Re < 21000	Kumar et al. [27]
d_B-7	$\frac{g\rho_L d_B^2}{\sigma} = 8.8 \left(\frac{u_G \mu_L}{\sigma} \right)^{-0.04} \left(\frac{\sigma^3 \rho_L}{g\mu_L^4} \right)^{-0.12} \left(\frac{\rho_L}{\rho_G} \right)^{0.22}$		Wilkinson et al. [28]

Table 1
Correlations for predicting bubble diameter (d_B)

Eq.	Correlation	Conditions	Reference
U_B-1	$U_B = \frac{g \cdot \Delta \rho \cdot d_B^2}{12 \cdot \mu_L}$	$Re < 250, \frac{\mu_G}{\mu_L} = 0$	Hadamard et Rybczynski [29]
U_B-2	$U_B = \frac{g \cdot \Delta \rho \cdot d_B^2}{18 \cdot \mu_L}$	$Re < 250, \frac{\mu_G}{\mu_L} \rightarrow \infty$	Frumkin et Levich [30]
U_B-3	$U_B = \frac{\mu_L}{\rho_L d_B} (J - 0.857) M_o^{-0.149}$ $J = 0.94 H^{0.757} \quad (2 < H \leq 59.3)$ $J = 0.32 H^{0.441} \quad (H > 59.3)$ $H = \frac{4}{3} E_o M_o^{-0.149} \left(\frac{\mu_L}{0.0009} \right)^{-0.14}$	$250 < Re < 6000$	Grace et al. [31]
U_B-4	$U_B = \left(\frac{2\sigma}{d_B \rho} + 0.5 d_B g \right)^{0.5}$	$0.2 \leq d_B \leq 8 \text{ cm}$	Mendelson [32]
U_B-5	Experimental curve for the bubble rising velocity		Grace & Wairegi [33]

Table 2
Correlations for predicting bubble rising velocity (U_B)

Moreover, according to the prediction of the liquid-side mass transfer coefficient (k_L), the literature [10], [11], [21], [22], [34], [35] related to k_L shows that the experimental k_L values vary between the two correlations:

$$\text{Higbie [35]:} \quad k_L = 2 \sqrt{\frac{D \cdot U_B}{\pi \cdot h}} \quad (6)$$

$$\text{Frossling [35]:} \quad k_L = \frac{D}{d_B} (2 + 0.6 \cdot Re^{\frac{1}{2}} \cdot Sc^{\frac{1}{3}}) \quad (7)$$

where h is the bubble height, close to its diameter at low gas flow rates. Re is the bubble Reynolds number and Sc is the Schmidt number. Normally, the Higbie's theory is valid for mobile spherical bubbles ($d_B > 2.5$ mm) having short contact times with the liquid, whereas the Frossling's equation deals with spherical bubbles having rigid interface ($0.1 \text{ mm} < d_B < 2$ mm).

3.2 The proposed theoretical $k_L a$ prediction method

In this present work, in order to obtain the $k_L a$ coefficient, the bubble size is considered as the initial parameter for calculating the others as bubble rising velocity, interfacial area and k_L coefficient: the existing correlations previously presented will be applied. Moreover, the predicted results are then compared with those obtained with the experimental process in a small-scale bubble column (Figure 1) for evaluating a range of such correlations to determine the preferred one, and thus providing finally the $k_L a$ values. The developed $k_L a$ prediction method can be thus described as follows:

- Calculating the bubble sizes generated by the industrial rubber membrane (d_B) used in this work (Table 1). Different correlations will be applied in the operating conditions corresponded to those used in this work, like hole diameter, orifice number, gas flow rate, pressure drop, etc;
- Determining the bubble formation frequency (f_B) by Equation (1), the bubble surface (S_B) and then the bubble rising velocity (U_B) related to the obtained bubble sizes and their operating conditions (Table 2);
- Calculating the values of interfacial area (a) by using Equation (3) and comparing with those obtained experimentally;
- Estimating the k_L coefficient by applying two of the most recommended equations: Higbie (1935) and Frossling (1938). Note that the bubble sizes and the operating conditions previously determined are used in this step.

- Determining finally the $k_L a$ coefficient as the product of the calculated values of (a) and the k_L coefficient.

IV. Results and Discussions

In this part, the experimental bubble hydrodynamic (d_B , f_B and U_B) and mass transfer parameters (a , k_L and $k_L a$) are compared with those predicted from existing correlations defined and numbered in Table 1 and 2. Moreover, the interfacial area and volumetric mass transfer coefficient will be determined and compared with the proposed method.

Figure 2
Comparison of experimental and predicted bubble sizes for the different flow rates

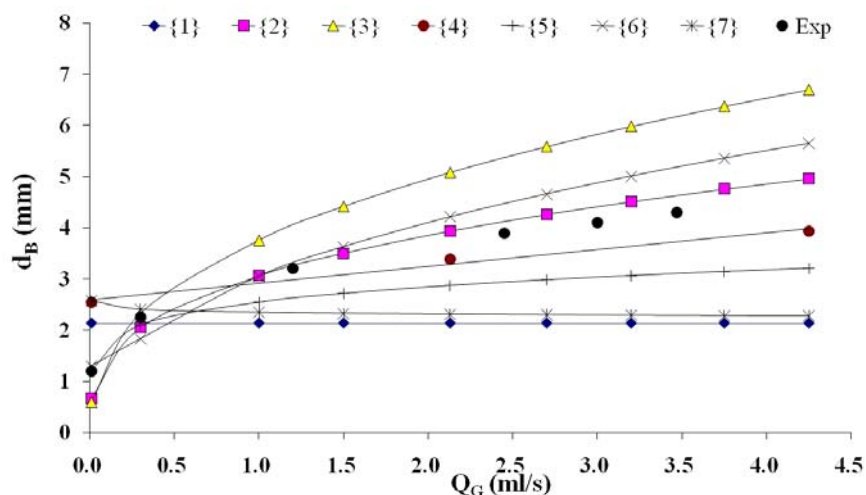
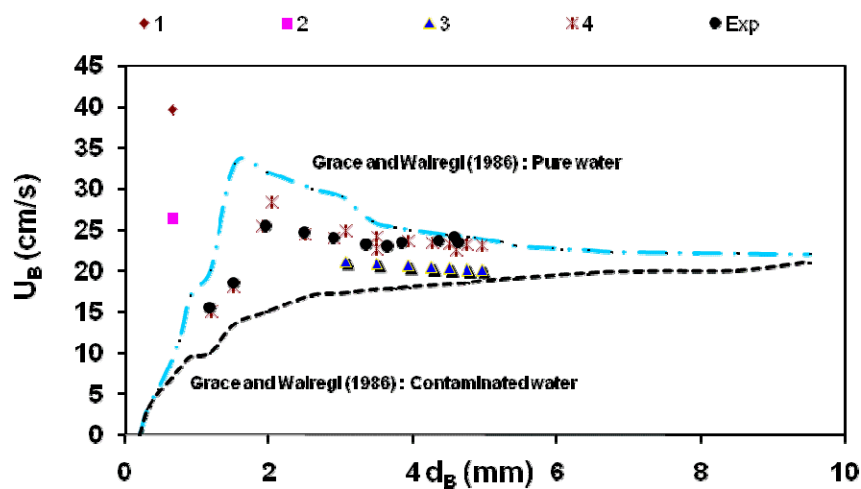


Figure 3
Comparison of experimental and predicted bubble rising velocity for different bubble diameters



4.1 Bubble hydrodynamic parameters

Bubble size generated by industrial rubber membrane (d_B)

Figure 2 presents the variation of the experimental and predicted bubble sizes (d_B) versus the gas flow rates. According to the hole expansion due to the membrane's elastic nature [9], the average hole diameter ($d_{OR} = 0.22$ mm) is chosen in order to calculate the value of d_B in this study.

According to Figures 2, the bubble diameters obtained experimentally vary between 0.45 and 4.5 mm while gas flow rates can change between 0.3 and 3.45 ml/s: the logarithmic increase in bubble diameter with a gas flow rate is observed. The results agree with the bubble generation phenomena, associated with membrane spargers [9, 22].

Concerning to the different correlations for predicting the bubble size, three trendlines can be observed as: 1) by applying the Equation (d_{B-1}), bubble size is independent to the gas flow rate 2) Bubble size decreases with the increase of the gas flow rate as obtained with Equation (d_{B-7}) and 3) Bubble size increase with the gas flow rate (Eq. (d_{B-2}) to (d_{B-6})): these tendency agrees with those obtained experimentally in this study. Therefore, it can be noted that, in order to determine the bubble size in this range of gas flow rate, the force balance at detachment (buoyancy force and surface tension force) and the associated physical characteristics of the system are likely not enough. On the other hand, the parameters relating to the power dissipated in the liquid phase that can render a condition in the bubble break up and coalescence, like pressure drop, gas flow rate, Reynolds number due to the membrane orifice (Re_{OR}), etc, should be also taken into account. Moreover, concerning to the bubble size prediction, a non-spherical bubble formation model at a flexible orifice has been proposed and also applied as the reliable method [6]. The predicted and the measured bubble diameters are in good agreement: the difference is below 15%. Note that this model has been firstly developed by Terasaka and Tsuge (1990) for rigid orifices and then adapted in the case of flexible orifice by taking into account the membranes features (elastic behavior and wettability).

According to the d_B values obtained with Equations (d_{B-2} to d_{B-6}), these exhibit a degree of scattering. This is due to the fact that the correlations are applied in this calculation base on different conditions like, the experimental set-up (gas sparger, bubble column size, etc), the operating conditions (temperature, pressure, etc) and also the bubble size measuring method. In this study, it can be found that the bubble sizes predicted by Leibson's correlation (Eq. (d_{B-2})) are close to those obtained experimentally in this work (average difference about $\pm 15\%$). Therefore, this correlation (Eq. (d_{B-2})) will be used as the initial parameter to determine the bubble rising velocity and then the mass transfer parameters in the following study.

Bubble rising velocity (U_B)

Figure 3 shows the variation of the experimental and predicted bubble rising velocity (U_B) versus the bubble diameter generated. The similar figure also presents the experimental U_B values obtained by Grace and Wairegi [39].

According to Figure 3, over the whole bubble diameter range (1 - 5 mm), the terminal rising bubble velocities (obtained experimentally) are nearly constant and ranged between 15 and 25 $\text{cm}\cdot\text{s}^{-1}$. Figure 3 shows that the terminal rising velocities obtained in this study lie within the range of the U_B values of Grace and Wairegi [33] corresponding to the contaminated and pure systems. The terminal rising bubble velocities obtained in water in this study are lower than those of pure water given by [33]. This difference is certainly due to the poor quality of the tap water used in this work ($\sigma_L \approx 71.8 \text{ mN/m}$).

In order to predict the values of U_B , the calculated bubble diameters are needed as presented in Table 1. It can be firstly noted that the Equations (U_{B-1}) and (U_{B-2}), which correspond to the spherical bubble that behaves like rigid spheres [36], can not be applied in this U_B calculation. On the other hand, according to the Equation (U_{B-3}) and (U_{B-4}), the average differences between the experimental and the predicted values are about $\pm 25\%$ and $\pm 15\%$ respectively. Due to the simple prediction process and also the possibility for determining U_B values in various contaminated liquid phases (effect of surface tension, σ_L), Mendelson's equation (Eq. U_{B-4}) is thus chosen for determining the bubble rising velocity in order to deduce then the interfacial area (a) from the values of d_B , f_B and U_B in this study.

4.2 Mass transfer parameters

Interfacial area (a)

The existing correlations used in this study to compare the predicted interfacial area (a) are presented in Table 3.

Note that, in order to calculate the values of a , the gas holdup (ε_G) are required. The gas holdup values are directly dependent on gas sparger types and physico-chemical properties of the liquid phase. It is a very important hydrodynamic parameter affecting the mass transfer mechanism in bubble columns. Therefore, in order to calculate the value of gas hold-up (ε_G), the ε_G values were based on the different correlations normally applied in bubble column and

presented in Table 4 [21]. In this work, the Joshi's correlation (Equation ε_G -1) are chosen due to the good first approximation and because there is no need the iterative solution methods as required by other correlations.

Table 3
Correlations for predicting interfacial area (a)

Eq.	Correlation	Reference
a-1	$a = 34.4 * U_G^{0.25} * \varepsilon_G$	Deckwer [11]
a-2	$a = 26. \left(\frac{L_R}{d_R} \right)^{-0.3} \left(\frac{\rho_L \cdot \sigma_L^3}{g \cdot \mu_L^4} \right)^{-0.003} * \varepsilon_G$	Gestrich and Krauss [37]
a-3	$a = \frac{6}{2.5} \cdot \left(\frac{\sigma_L}{\rho_L \cdot g} \right)^{-0.5} \cdot \left(\frac{\mu_L \cdot U_G}{\sigma_L} \right)^{0.25} \cdot \left(\frac{\rho_L \cdot \sigma_L^3}{g \cdot \mu_L^4} \right)^{0.125} \cdot \varepsilon_G$	Van dierendonck et al. [38]
a-4	$a = 4.65 * 10^{-12} * \left(\frac{U_G}{\mu_L} \right)^{0.51}$	Tomida et al. [39]
a-5	$a = \frac{6\varepsilon_G}{d_B(1-\varepsilon_G)}$	Moustiri [40]
a-6	$a = 8.54 * U_G^{0.12} * \varepsilon_G$	Deckwer [11]

Table 4
Correlations for predicting gas holdup (ε_G)

Eq.	Correlation	Reference
ε_G -1	$\varepsilon_G = \frac{U_G}{0.3 + 2 \cdot U_G}$	Joshi and Sharma [41]
ε_G -2	$\varepsilon_G = \frac{U_G}{31 + \beta \cdot (1 - e) \cdot \sqrt{U_G}}$ $\beta = 4.5 - 3.5 \cdot \exp(-0.064 \cdot d_B^{1.3})$ $e = -0.18 \cdot U_G^{1.8} / \beta$	Joshi and Shah [42]
ε_G -3	$U_G \cdot (1 - \varepsilon_G) + U_L \cdot \varepsilon_G = U_B \cdot \varepsilon_G \cdot (1 - \varepsilon_G)^{2.39} (1 + 2.55 \cdot \varepsilon_G^3)$	Lockett and Kirkpatrick [43]
ε_G -4	$\varepsilon_G = 0.91 \cdot U_G^{1.19} / \sqrt{g \cdot d_B}$	Winkler [44]
ε_G -5	$\frac{U_G}{\varepsilon_G} + \frac{V_L}{1 - \varepsilon_G} = \frac{3 \cdot V_B \cdot (1 - \varepsilon_G) / (1 - \varepsilon_G^{5/3})}{1 + (2 + 3 \cdot \gamma / \mu_L) \cdot (1 - 0.628 / \sqrt{Re})}$	Kulkarni et al. [45]

According to the prediction of interfacial area used in the theoretical model, the Equation (3) is used in this study. The value of (a) links to the bubble diameter (d_B), the bubble formation frequency (f_B) as presented in equation 1 by assuming the constant bubble size generated, and the terminal rising bubble velocity results (U_B). Therefore, the predicted values of (a) in this part are calculated by using the values of d_B , f_B and U_B based on the Equation (d_B -1), (1) and (U_B -4) respectively. Figure 4 presents the variation of the experimental and predicted interfacial area (a) with the gas flow rates.

As shown in Figures 4, the interfacial area (obtained experimentally) roughly increases linearly with the gas flow rate. Their values vary between 1.8 and 13 m^{-1} whereas the gas flow rates change between 0.3 and 3.45 ml/s. In order to firstly predict the present experimental results, the existing correlations of interfacial area as presented in Table 3 were applied with the gas holdup obtained with the Equation (ε_G -1). Except for the results relating to Equation (a-5), the predicted (a) values are significantly smaller than those obtained experimentally: the noteworthy differences are observed. Thus, it can be noted that these existing correlations are not adequate to predict correctly the (a) values: diminutive

values of ε_G due to the actual small-scale aeration system used in this work is probably responsible for these consequences.

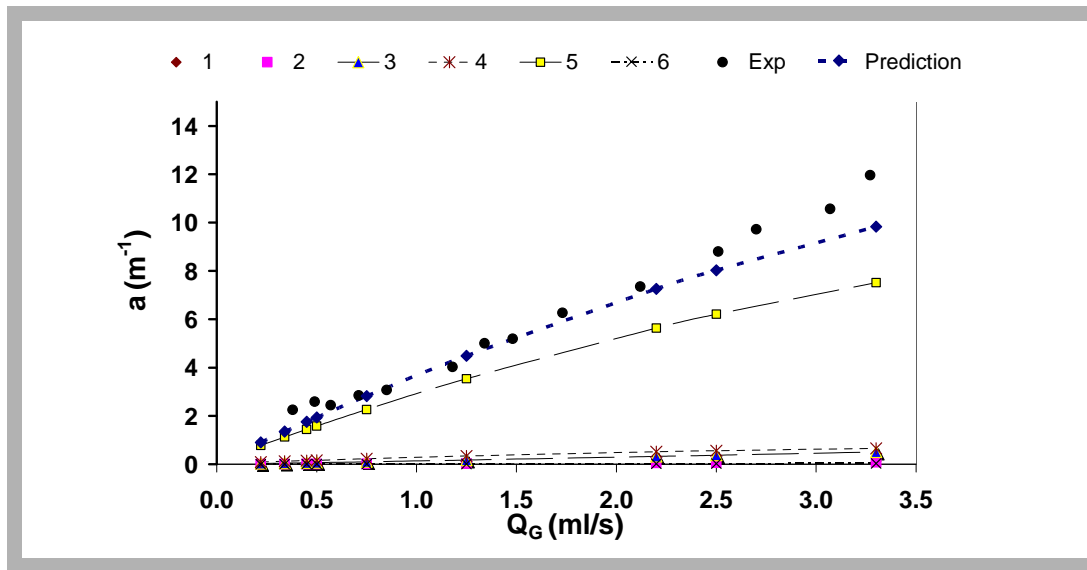


Figure 4
Comparison of experimental and predicted interfacial area for the different gas flow rates

On the other hand, due to the application of the calculated bubble diameter and the associated bubble rising velocity previously discussed, a quite good agreement between the experimental and the predicted values of (a) is obtained. The average difference about $\pm 15\%$ corresponds to the experimental error obtained in this study. However, for higher gas flow rates, this proposed method under-predicted the interfacial area: this should be due to the shape modification (change from the spherical shape to the ellipsoidal shape). Therefore, the surface area of an ellipsoidal bubble should be applied in order to correct this observed differences.

Therefore, it can be concluded that, as known the bubble diameter generated (assumed to be constant) and their associated rising velocity, it is possible to predict simply the interfacial area. However, more experimental data are necessary to validate this method: in the future, different contaminants presence in the liquid phase and gas sparger effect will be tested to extend the operating condition ranges. Furthermore, the effect of the membrane's hole diameter (d_{OR}) and also bubble shape modification will be carefully studied to improve the modeling and hence to provide a better understanding of the gas-liquid aeration mechanisms.

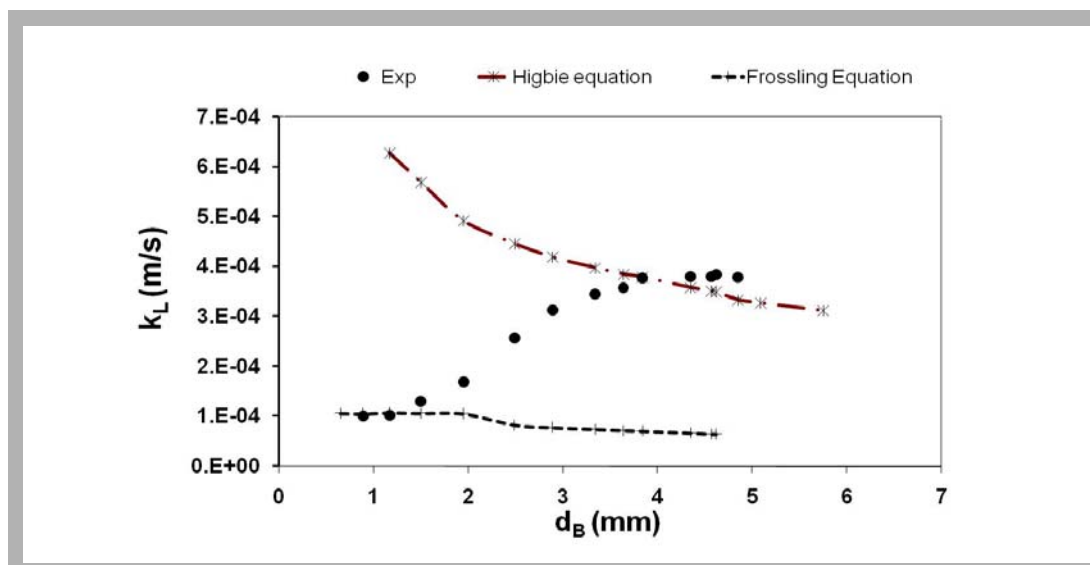


Figure 5
Comparison of experimental and predicted liquid-side mass transfer coefficient for different bubble diameters

Liquid-side mass transfer coefficient (k_L)

Figure 5 shows the variation of the experimental and predicted liquid-side mass transfer coefficient (k_L) with the bubble diameter generated. In order to predict this value, two equations (Higbie (1935) and Frossling (1938)) are applied in this study.

Eq.	Correlation	Reference
k_La-1	$k_L a = 0.0269 * U_G^{0.82}$	Deckwer et al. [46]
k_La-2	$k_L a = d_C^{0.17} * U_G^{0.7}$	Akita and Yoshida [47]
k_La-3	$\frac{k_L a}{U_G} \cdot \left(\frac{v_L^2}{g}\right)^{0.33} = 3.9 \cdot 10^{-5} * \left[\frac{\mu_G}{(v_L \cdot g)^{0.33}}\right]^{-0.1}$	Zlakarnik [48]
k_La-4	$k_L a = 0.041 \cdot \alpha \cdot \left(\frac{H_L}{d_B^{0.67}}\right) \cdot \left(\frac{d_{OR}}{D_C}\right)^{0.18} \cdot \left(\frac{U_G}{H_L}\right)$	Khudenko and Shpirt [49]
k_La-5	$k_L a = f_C \cdot \sqrt{\frac{4 \cdot D \cdot R_{sf}}{\pi \cdot S_B} \cdot \frac{f_B \cdot S_B}{A \cdot U_B}}$ $f_C = 0.211 E o^{0.63}$ $R_{sf} = \pi \cdot \sqrt{\frac{l^2 + h^2}{2} - \frac{l^2 - h^2}{8}} \times U_B$	Nedeltchev et al. [50]

Table 5
Correlations for predicting volumetric mass transfer coefficient ($k_L a$)

From the Figure 5, the k_L values (obtained experimentally) vary between 0.00015 and 0.00042 $m \cdot s^{-1}$ for bubble sizes varying between 1 and 5 mm. Moreover, it can be noted that the k_L values remain roughly constant for bubble diameters less than 1.5 mm and greater than 3.5 mm. For bubble diameters varying between 1.5 mm and 3.5 mm, an increase in the k_L values is observed. The results in this study agree with the three zones of the k_L coefficients proposed by [10].

According to a comparison between these two models and the present experimental results, the following comments can be made:

- the k_L values obtained with Higbie's equation are close to those obtained experimentally at the bubble diameter greater than 3.5 mm, but significant differences appear at larger d_B . The ellipsoid bubble shape is probably responsible for these results;
- the k_L values deduced from the Frossling equation are quite similar to those obtained experimentally at small bubble diameters ($d_B < 1.5$ mm), but they diverge at larger d_B ;
- for the bubble diameter between 1.5 and 3.5 mm, the existing models can not predict correctly the k_L values. This is probably due to the variation of k_L values which corresponds to the modification of the bubble shape from spherical to ellipsoidal occurred in this bubble range [10], [51].

Therefore, the gap of existing models consists mainly not in taking sufficiently into account the geometrical transition from the spherical shape to the ellipsoidal shape on the k_L coefficients. Due to this difficulty, it can cause surely the inaccuracy onto the prediction of the associated $k_L a$ coefficient in the following study.

Volumetric mass transfer coefficient ($k_L a$)

In this part, the experimental results are firstly compared with those obtained with the different existing correlations (Table 5).

The correlations are applied by considering the same parameters associated with the operating conditions and physical characteristics used in this study. A small effective limit placed on the resulting application is assumed. Moreover, it can be expressed that all the $k_L a$ correlations were developed concerning to the clean system (clean water), with no contaminations. Khudenko and Shpirt' equation (Eq. $k_L a-4$) is the exception here: the α -factor, which is a ratio of processing water to clean water volumetric

mass transfer coefficients, or $\frac{k_L a_{\text{Process water}}}{k_L a_{\text{Clean water}}}$, is added in order to consider the effect of

different contaminants presence in liquid phases. Note that the value of α -factor is equal to 1 in this study. Figure 6 presents the variation of the experimental and predicted volumetric mass transfer coefficient ($k_L a$) with the gas flow rates for existing correlations (Table 5).

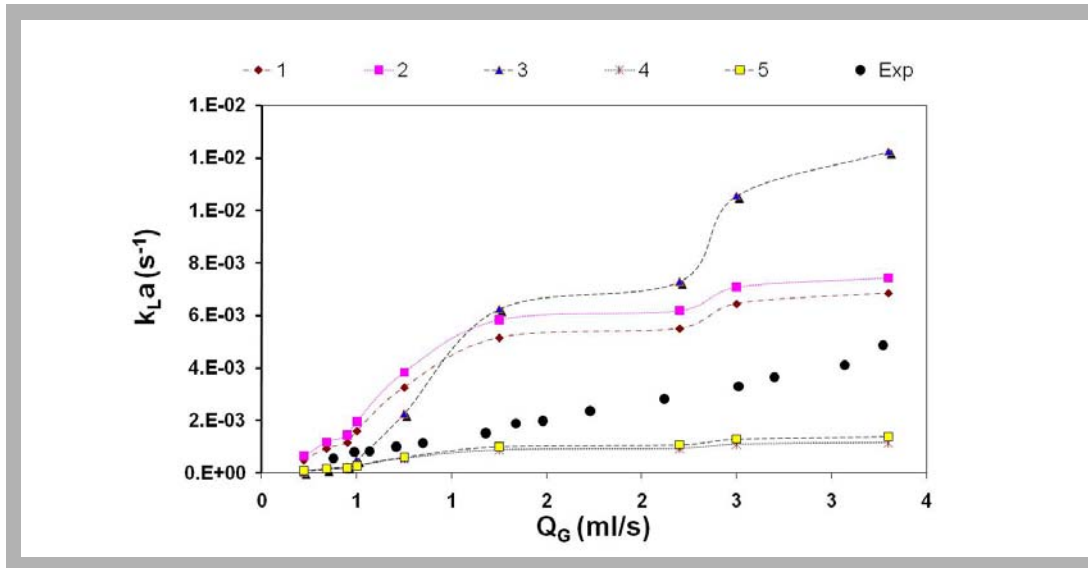


Figure 6
Comparison of experimental and predicted volumetric mass transfer coefficient ($k_L a$) by using the existing correlations for the different gas flow rates

This last figure indicates that, the volumetric mass transfer coefficient (obtained experimentally) increases with the gas flow rate, which in turn systematically induces an increase in either interfacial area (a) or liquid-side mass transfer coefficient (k_L). The values of $k_L a$ vary between 0.00035 and 0.0045 s^{-1} , for gas flow rates varying between 0.3 and 3.45 ml/s. According to the comparison between the experimental and calculated results, the calculated $k_L a$ values also increase with the gas flow rate, whereas the momentous differences from the experimental ones are observed. This is because the $k_L a$ coefficient, which depends on many associated parameters, are normally used for considering the oxygen transfer rather in global system than in local system as in this study. Moreover, in order to obtain correctly the assumption concerning to the respond time of the oxygen probe and the perfectly mixed condition of the liquid phase as in classical method is needed.

Recently, Painmanakul et al. [22] have proposed for a bubble train provided in a small bubble column a new $k_L a$ experimental method based on the mass balance on the quantity of sodium sulphite consumed during an aeration step: no assumption concerning to the respond time of the oxygen probe and the perfectly mixed condition of the liquid phase.

Moreover, only specific operating condition is probably suitable for each existing correlation. Thus, it can be expressed that the correlations could not be applied to predict the values of $k_L a$ obtained in this study.

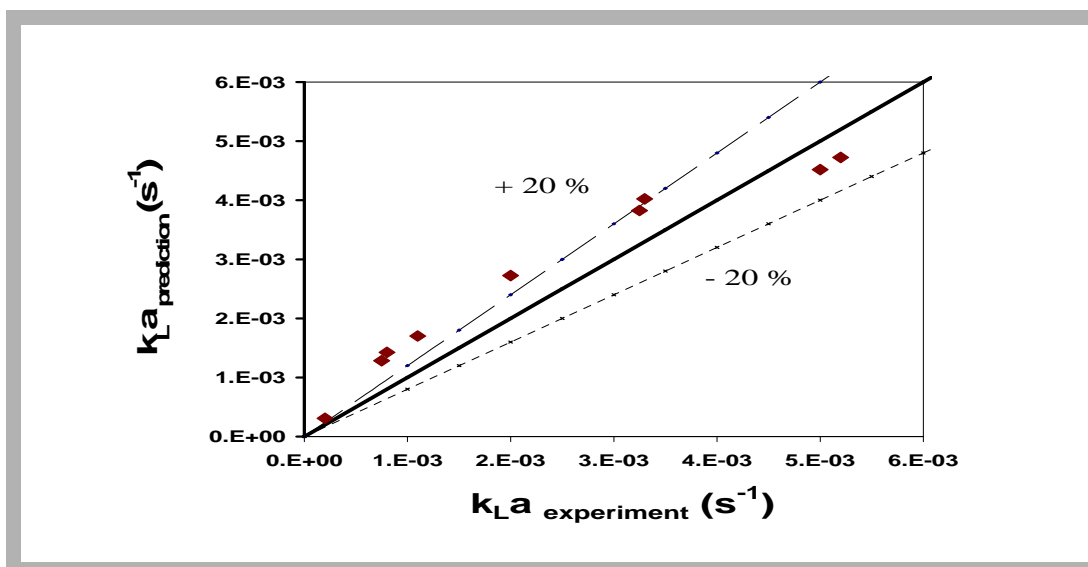


Figure 7
Comparison of experimental and predicted volumetric mass transfer coefficient ($k_L a$) by using the existing correlations for the different gas flow rates

Prediction of the $k_L a$ coefficient based on the proposed method

In order to understand and predict correctly the $k_L a$ values, both interfacial area (a) and the liquid-side mass transfer coefficient (k_L) is therefore interesting to be taken into account.

In this study, the predicted $k_L a$ coefficient is thus calculated as the product of the calculated values of (a) and of k_L coefficient. The values of (a) are determined, in this part, by using the values of d_B and U_B based on the Equation (d_B -1) and (U_B -4) respectively. Moreover, the bubble diameter equal to 1.5 mm is considered for selecting the k_L models between Higbie and Frossling equations in order to calculate finally the $k_L a$ coefficient (Frossling equations used for $d_B < 1.5$ and Higbie equations used for $d_B > 1.5$).

Note that the prediction of $k_L a$ accumulates the errors associated with both values of (a) and k_L previously presented. The average calculated error has been estimated at $\pm 20\%$, which corresponds to the experimental error obtained with the $k_L a$ measured method [22].

Figure 7 shows that a relatively good agreement between the experimental and the predicted $k_L a$ coefficient is obtained (average difference about $\pm 20\%$). However, the significant differences appear at the intermediate values of $k_L a$ coefficient: the inadequacy due to the application of the Higbie's and Frossling's models as previously presented is probably responsible for these consequences.

Therefore, in the future, the effect of geometrical transition from the spherical shape to the ellipsoidal shapes should be considered in order to predict properly the k_L coefficients range between 1.5 and 3.5 mm. More experimental data are necessary to accurately validate this method and other mixtures of various contaminants and different gas spargers should be tested to extend the operating conditions. However, the idea to predict on the one side the interfacial area from equation (3) using literature correlations and on the other side to predict the liquid-side mass transfer coefficient allowed obtaining the volumetric mass transfer coefficient ($k_L a$) for a gas-liquid contactor with a good accuracy.

V. Conclusions

The objective of this work was to propose the new theoretical prediction method of the volumetric mass transfer coefficient ($k_L a$) based on the dissociation of the parameters, especially the liquid-side mass transfer coefficient (k_L) and the interfacial area (a). Furthermore, the following results have been obtained:

- The generated bubble sizes (d_B) can be used as the key factor in order to predict, not only the $k_L a$ coefficient, but also both values of a and k_L within the associated operating conditions;
- The interfacial area links to the bubble diameter (d_B), the bubble formation frequency (f_B) and the terminal rising bubble velocity results (U_B). Therefore, by predicting the values of d_B and U_B based on the Leibson's correlation [25] and Mendelson's correlation [32] respectively, it is possible to predict the interfacial area with the average differences between the predicted and experimental results about $\pm 15\%$;
- The existing models (Higbie's and Frossling's equations) cannot be applied to predict correctly the k_L values for the bubble diameter between 1.5 and 3.5 mm, This is probably due to the variation of k_L values which corresponds to the modification of the bubble shape from spherical to ellipsoidal occurred in this bubble range;
- The existing correlations cannot be used to predict the values of $k_L a$ obtained with local system as in this study, on the other hand, the proposed theoretical prediction method has allowed a relative good coincidence between the experimental and predicted $k_L a$ coefficient to be obtained (average difference about $\pm 20\%$); It can be supposed that its application to global systems can be interesting to well predict the volumetric mass transfer values provided in gas-liquid contactors.

In the future, the effect of the modification of the bubble shape (spherical to ellipsoidal) will be essential to take into account for improving the determination of (a) and k_L values, hence the predicted $k_L a$ coefficient. In addition, it is obvious that the results observed in our little bubble column volume have to be validated into a tall bubble column and at higher gas flow rates. Finally, in order to validate the $k_L a$ predicting correlation proposed in this study, more experimental data are necessary with other liquid phases and different gas spargers to extend the operating condition ranges such as the aqueous solutions with surfactants and also the industrial and/or urban wastewaters.

Notation

A	cross-sectional area of reactor	[m ²]
A _B	bubble area	[m ²]
a	interfacial area	[m ⁻¹]
C _L	dissolved oxygen concentration	[kg/m ³]
C _L [*]	oxygen concentration at saturation	[kg/m ³]
C	solute concentration in liquid phase	[kg/m ³]
CMC	Critical Micelle Concentration	[kg/m ³]
d _B	bubble diameter	[m]
D _C	bubble column diameter	[m]
D _{OR}	equivalent hole diameter	[m]
D	gas diffusivity coefficient in water, m ² .s ⁻¹	
E	bubble eccentricity	[-]
f _B	bubble formation frequency	[s ⁻¹]
g _c	acceleration due to gravity	[m/s ²]
H	dimensionless group defined in Equation (U _B -3)	[-]
H _L	liquid height	[m]
J	dimensionless group defined in equations (U _B -3)	[-]
K	adsorption constant at the equilibrium	[m ³ /mol]
k _L	liquid-side mass transfer coefficient	[m/s]
k _{La}	volumetric mass transfer coefficient	[s ⁻¹]
M	molecular mass	[kg/mol]
m _R	mass of Na ₂ SO ₃ remaining in the column	[kg]
m _S	mass of Na ₂ SO ₃ reacting with the dissolved oxygen	[kg]
m _T	total mass of Na ₂ SO ₃ introduced initially	[kg]
N _B	number of bubbles generated	[-]
N _{OR}	number of orifice	[-]
q	gas flow rate through the orifice	[m ³ /s]
Q _G	gas flow rate	[m ³ /s]
S _B	total bubble surface	[m ²]
t _{Aeration}	aeration time	[s]
T _{frame}	time between two frames, s	
T	temperature	[°C]
U _B	bubble rising velocity	[m/s]
U _G	superficial gas velocity	[m/s]
V _C	gas chamber volume between the control valve and the orifice	[m ³]
V _B	bubble volume	[m ³]
V _L	liquid volume in reactor	[m ³]
V _{Total}	total volume in reactor	[m ³]

Dimensionless numbers

Eo	Eötvös number defined by	$Eo = g(\rho_L - \rho_G)d_B^2 / \sigma_L$	[-]
Mo	Morton number defined by	$Mo = (g\mu_L^4(\rho_L - \rho_G)) / (\rho_L^2\sigma_L^3)$	[-]
Re	Bubble Reynolds number defined by	$Re = U_B \cdot \rho_L \cdot D_B / \mu_L$	[-]
Re _{OR}	Hole Reynolds number defined by	$Re = U_G \cdot \rho_G \cdot D_{OR} / \mu_G$	[-]
Sc	Schmidt number defined by	$Sc = \mu_L / (\rho_L D)$	[-]
We	Weber number defined by	$We = U_G^2 \cdot d_{OR} \cdot \rho_G / \sigma_L$	[-]

Greek symbols

ΔD	bubble spatial displacement between two frames	[m]
ΔP	pressure drop	[Pa]
α	ratio of volumetric mass transfer coefficient in liquid to that in tap water	[-]
ε _G	Gas hold-up	[-]
μ _L	liquid viscosity	[Pa.s]
ν _L	kinematic viscosity	[m ² /s]
ρ _G	gas density	[kg/m ³]
ρ _L	liquid density	[kg/m ³]
σ _L	liquid surface tension	[N/m]

REFERENCES

- [1] D. J. Reardon, "Turning down the power," *Civil Engineering*, vol. 65, no. 8, pp. 54-56, 1995.
- [2] R. G. Rice and N. B. Lakhani, "Bubble formation at a puncture in a submerged rubber membrane," *Chemical Engineering Communications*, vol. 24, no. 4-6, pp. 215-234, 1983.
- [3] R. G. Rice and S. W. Howell, "Elastic and flow mechanics for membrane spargers," *AIChE Journal*, vol. 32, no. 8, pp. 1377-1382, 1986.
- [4] R. G. Rice, J. M. I. Tupperainen and R. Hedge, "Dispersion and hold up in bubble columns: Comparison of rigid and flexible sparger," *The Canadian Journal of Chemical Engineering*, vol. 59, no. 6, pp. 677-687, 1981.
- [5] F. Bischof and M. Sommerfeld, *Studies of the Bubble Formation Process for Optimisation of Aeration Systems*. Tsukuba, Japan, September, 1991.
- [6] K. Loubière and G. Hébrard, "Bubble formation from a flexible hole submerged in an inviscid liquid," *Chemical Engineering Science*, vol. 58, no. 1, pp. 135-148, 2003.
- [7] G. Hébrard, D. Bastoul and M. Roustan, "Influence of the gas spargers on the hydrodynamic behaviour of bubble columns," *Transactions. Institution of Chemical Engineers*, vol. 74, no. 3, pp. 406-414, 1996.
- [8] P. Painmanakul, K. Loubière, G. Hébrard and P. Buffière, "Study of different membrane spargers used in waste water treatment: Characterisation and performance," *Chemical Engineering and Processing*, vol. 43, no. 11, pp. 1347-1359, 2004.
- [9] R. Sardeing, P. Painmanakul and G. Hébrard, "Effect of surfactants on liquid-side mass transfer coefficients in gas-liquid systems: A first step to modeling," *Chemical Engineering Science*, vol. 61, no. 19, pp. 6249-6260, 2006.
- [10] P. Painmanakul and G. Hébrard, "Effect of different contaminants on the α -factor: Local experimental method and modeling," *Chemical Engineering Research and Design*, vol. 86, no. 11, pp. 1207-1215, 2008
- [11] W. D. Deckwer, *Bubble Column Reactors*. Chichester: John Wiley, 1992.
- [12] M. Roustan, "Coefficient de transfert et modèle de transferts" in: *Roustan, M. (Ed.), Transferts gaz-liquide dans les procédés de traitement des eaux et des effluents gazeux*. Lavoisier, Paris, 1978.
- [13] G. Vázquez, M. A. Cancela, R. Varela, E. Alvarez and J. M. Navaza, "Influence of surfactants on absorption of CO₂ in a stirred tank with and without bubbling," *Chemical Engineering Journal*, vol. 67, no. 2, pp. 131-137, 1997.
- [14] C. Akosman, R. Orhan and G. Dursun, "Effects of liquid property on gas holdup and mass transfer in co-current downflow contacting column," *Chemical Engineering and Processing*, vol. 43, no. 4, pp. 503-509, 2004.
- [15] M. Bouaifi, G. Hébrard, D. Bastoul and M. Roustan, "A comparative study of gas hold-up, bubble size, interfacial area and mass transfer coefficients in stirred gas-liquid reactors and bubble columns," *Chemical Engineering and Processing*, vol. 40, no. 2, pp. 97-111, 2001.
- [16] B. Zhao, J. Wang, W. Yang and Y. Jin, "Gas-liquid mass transfer in slurry bubble systems: I. Mathematical modeling based on a single bubble mechanism," *Chemical Engineering Journal*, vol. 96, no. 1-3, pp. 23-27, 2003.
- [17] B. Zhao, J. Wang, W. Yang and Y. Jin, "Gas-liquid mass transfer in slurry bubble systems: II. Verification and simulation of the model based on the single," *Chemical Engineering Journal*, vol. 96, no. 1-3, pp. 29-35, 2003.
- [18] J. M. T. Vasconcelos, J. M. L. Rodrigues, S. C. P. Orvalho, S. S. Alves, R. L. Mendes and A. Reis, "Effect of contaminants on mass transfer coefficients in bubble column and airlift contactors," *Chemical Engineering Science*, vol. 58, no. 8, pp. 1431-1440, 2003.
- [19] G. Vázquez, M. A. Cancela, C. Riverol, E. Alvarez and J. M. Navaza, "Application of the danckwerts method in a bubble column: Effects of surfactants on mass transfer coefficient and interfacial area," *Chemical Engineering Journal*, vol. 78, no. 1, pp. 13-19, 2000.
- [20] A. H. G. Cents, D. W. F. Brillman and G. F. Versteeg, "Gas absorption in an agitated gas-liquid-liquid system," *Chemical Engineering Science*, vol. 56, no. 3, pp. 1075-1083, 2001.
- [21] J. Dudley, "Mass transfer in bubble columns: A comparison of correlations," *Water Research*, vol. 29, no. 4, pp. 1129-1138, 1995.
- [22] P. Painmanakul, K. Loubière, G. Hébrard, M. Mietton-Peuchot and M. Roustan, "Effects of surfactants on liquid-side mass transfer coefficients," *Chemical Engineering Science*, vol. 60, no. 22, pp. 6480-6491, 2005.
- [23] E. L. Schierholz, J. S. Gulliver, S. C. Wilhelms and H. E. Henneman, "Gas transfer from air diffusers," *Water Research*, vol. 40, no. 5, pp. 1018-1026, 2006.
- [24] W. V. Krevelen and M. J. Jackson, *Industrial Engineering Chemical Program*, vol. 46, p. 29, 1959.
- [25] I. Leibson, E. G. Helcomb, A. G. Cocosco and J. J. Jacmie, "Rate of flow and mechanics of bubble formation from single submerged orifices. I. Rate of flow studies," *AIChE Journal*, vol. 2, no. 3, pp. 296-300, 2004.
- [26] G. Hebrard, *Etude de l'influence du distributeur de gaz sur l'hydrodynamique et le transfert de matière gaz-liquide des colonnes à bulles*, INSA Toulouse, 1995.
- [27] A. Kumar, T. E. Delgaleesan, G. S. Laddha and H. E. Hoelscher, "Bubble swarm characteristics in bubble columns," *Canadian Journal of Chemical Engineering*, vol. 54, no. 6, pp. 503-508, 2009.
- [28] P. M. Wilkinson, H. Haringa and L. L. V. Dierendonck, "Mass transfer and bubble size in a bubble column under pressure," *Chemical Engineering Science*, vol. 49, no. 9, pp. 1417-1427, 1994.
- [29] J. S. Hadamard and Ryazantsev, "Mouvement permanent lent d'une sphere liquide et visqueuse dans un liqeué visqueux," *Comptes rendus de l'Académie des sciences*, vol. 152, pp. 1735-1738, 1911.
- [30] A. Frumkin and V. G. Levich, "On surfactants an interfaciale motion," *Zh. Fiz. Khim*, vol. 21, pp. 1183 - 1204, 1947.
- [31] J. R. Grace, T. Wairegi and T. H. Nguyen, "Shapes and velocities of single drops and bubbles moving freely through immiscible liquids," *Transactions of the Institution of Chemical Engineering*, vol. 54, pp. 167-173, 1976.
- [32] H. D. Mendelson, "The prediction of bubble terminal velocities from wave theory," *AIChE Journal*, vol. 13, pp. 250-253, 1967.
- [33] J. R. Grace and T. Wairegi, "Properties and Characteristics of Drops and Bubbles", in the *Encyclopedia of Fluid Mechanics, Cheremisinoff.Chap 3*, Gulf Publishing, Huston: TX, 1986.
- [34] G. Hebrard, P. Destrac, M. Roustan, A. Huyard, and J. M. Audic, "Determination of the water quality correction factor using a tracer gas method," *Water Research*, vol. 24, no. 2, pp. 684-689, 2000.
- [35] M. Roustan, *Transferts gaz-liquide dans les procédés de traitement des eaux et des effluents gazeux*: TEC&DOC, 2003.
- [36] R. E. Treybal, *Mass Transfer Operations*. New York: McGraw-Hill, 1980.
- [37] W. Gestrich and W. Krauss, "Die spezifische phasengrenzfläche in blasensäulen (The specific interfacial area in bubble columns)," *Chemie Ingenieur Technik*, vol. 47, pp. 360-367, 1975.
- [38] L. J. V. Dierendonck, J. M. Fortuin and D.Venderbos, *Proceedings of the 4th European Symposium on Chemical Reaction Engineering*. Brussels, 1968.
- [39] T. Tomida, F. Yusa and T. Okazaki, "Effective interfacial area and liquid-side mass transfer coefficient in the upward two-phase flow of gas-liquid mixtures," *Chemical Engineering Journal*, vol. 16, no. 2, pp. 81-88, 1978.
- [40] S. Moustiri, "Hydrodynamique des colonnes à bulles fonctionnant à co-courant de gaz et de liquide: Effet hydrodynamique produit par la présence d'un garnissage spécifique Thèse N°601," INSA Toulouse, 2000.
- [41] J. B. Joshi and M. M. Sharma, "A circulation model for bubble columns," *Transactions of the Institute of Chemical Engineers*, vol. 57, pp. 244-251, 1979.
- [42] J. B. Joshi and Y. T. Shah, "Invited review hydrodynamic and mixing models for bubble column reactors," *Chemical Engineering Communications*, vol. 11, no. 1-3, pp. 165-199, 1981.

- [43] M. J. Lockett and R. D. Kirkpatrick, "Ideal bubbly flow and actual flow on bubble columns," *Transactions of the Institute of Chemical Engineers*, vol. 53a, pp. 267-273, 1975.
- [44] M. Winkler, *Biological Treatment of WasteWater*. Chichester: Elliss Horwood, 1981.
- [45] A. Kulkarni, Y. T. Shah and B. G. Kelkar, "Gas hold-up in bubble column with surface-active agents: A theoretical model," *AIChE Journal*, vol. 33, pp. 690-693, 1987.
- [46] W. D. Deckwer, R. Burckart and G. Zoll, "Mixing and mass transfer in tall bubble column," *Chemical Engineering Science*, vol. 29, no. 11, pp. 2177 - 2188, 1974.
- [47] K. Akita and F. Yoshida, "Gas holdup and volumetric mass transfer coefficient in bubble columns," *Industrial and Engineering Chemistry Process Design and Development*, vol. 12, no. 1, pp. 76-80, 1973.
- [48] M. Zlakarnik, "Reactive red azo dye degradation in a UASB bioreactor: Mechanism and kinetic," *Acta Biotechnologica*, vol. 1, pp. 311-316, 1981.
- [49] B. M. Khudenko and E. Shpirt, "Hydrodynamic parameters of diffused air systems," *Water research*, vol. 20, no. 7, pp. 905-915, 1986.
- [50] S. Nedeltchev, U. Jordan and A. Schumpe, "A new correction factor for theoretical prediction of mass transfer coefficient in bubble columns," *Journal of Chemical Engineering of Japan*, vol. 39, pp. 1237-1242, 2006.
- [51] P. H. Calderbank and M. B. Moo-Young, "The continuous phase heat and mass-transfer properties of dispersions," *Chemical Engineering Science*, vol. 16, no. 1-2, pp. 39-54, 1961.
- [52] C. D. DeMoyer, E. L. Schierholz, J. S. Gulliver and S. C. Wilhelms, "Impact of bubble and free surface oxygen transfer on diffused aeration systems," *Water Research*, vol. 37, no. 8, pp. 1890-1904, 2003.
- [53] D. F. McGinnis and J. C. Little, "Predicting diffused-bubble oxygen transfer rate using the discrete-bubble model," *Water Research*, vol. 36, no. 18, pp. 4627-4635, 2002.
- [54] M. Roustan, *Quels sont les critères d'extrapolation pour les systèmes d'aération?* Tribune de l'Eau 1, 1996.
- [55] M. Zlokarnik, "Sorption characteristics of slot injectors and their dependency on the coalescence behaviour of the system," *Chemical Engineering Science*, vol. 34, no. 10, pp. 1265-1271, 1979.
- [56] S. Capela, M. Roustan and A. Héduit, "Transfer number in fine bubble diffused aeration systems," *Water Science and Technology*, vol. 43, no. 11, pp. 145-152, 2001.
- [57] S. Gillot, S. Capela-Marsal, M. Roustan and A. Héduit, "Predicting oxygen transfer of fine bubble diffused aeration systems-model issued from dimensional analysis," *Water Research*, vol. 39, no. 7, pp. 1379-1387, 2005.